Wind and Structures, Vol. 11, No. 3 (2008) 209-220

DOI: http://dx.doi.org/10.12989/was.2008.11.3.209

Effect of rain on flutter derivatives of bridge decks

Ming Gu* and Shu-zhuang Xu

State Key Laboratory for Disaster Reduction in Civil Engineering, Tongji University, Shanghai, 200092, P. R. China

(Received August 13, 2007, Accepted April 14, 2008)

Abstract. Flutter derivatives provide the basis of predicting the critical wind speed in flutter and buffeting analysis of long-span cable-supported bridges. Many studies have been performed on the methods and applications of identification of flutter derivatives of bridge decks under wind action. In fact, strong wind, especially typhoon, is always accompanied by heavy rain. Then, what is the effect of rain on flutter derivatives and flutter critical wind speed of bridges? Unfortunately, there have been no studies on this subject. This paper makes an initial study on this problem. Covariance-driven Stochastic Subspace Identification (SSI in short) which is capable of estimating the flutter derivatives of bridge decks from their steady random responses is presented first. An experimental set-up is specially designed and manufactured to produce the conditions of rain and wind. Wind tunnel tests of a quasi-streamlined thin plate model are conducted under conditions of only wind action and simultaneous wind-rain action, respectively. The flutter derivatives are then extracted by the SSI method, and comparisons are made between the flutter derivatives under the two different conditions. The comparison results tentatively indicate that rain has non-trivial effects on flutter derivatives, especially on H_2^* and A_2^*, and thus the flutter critical wind speeds of bridges.

Keywords: bridge deck; flutter derivative; rain and wind action; stochastic subspace identification.

1. Introduction

It has been recognized that wind induced vibrations of long-span bridges mainly include buffeting response due to wind turbulence and self-excited vibrations, such as flutter, vortex shedding and galloping. Among these flutter and buffeting responses are the most serious problems, and should be carefully checked through wind tunnel tests and analyses before the structural design of such bridges to ensure the safety during construction and operation stages.

In fact, strong wind, especially typhoon, is always accompanied by heavy rain. Then, what is the effect of rain on flutter critical wind speed and buffeting response of bridges? Unfortunately, there have been no studies on this subject. When the authors made analytical studies on rain-wind induced vibration of stay cables (Gu and Lu 2001), the air density was replaced by the mixture density of air and rain. This reminded the authors that rain might have non-trivial effects on loads acting on large structures, such as tall buildings and long-span bridges, although the mechanism may be entirely different from that of rain-wind induced vibration of stay cables, which has been

* Corresponding Author, E-mail: minggu@mail.tongji.edu.cn

deemed as the occurrence of an upper water rivulet and its vibration on the cable. In view of this consideration, a wind tunnel test on the flutter derivatives of a thin plate model is thus carried out under conditions of rain and wind as the first phase of the study to investigate the effects of rain and wind loads on structures.

Up to now, many studies have been performed on the methods and applications of identification of flutter derivatives of bridge decks under actions of wind forces (Scanlan and Lin 1978, Sarkar 1994, Gu, *et al*. 2000, Gu, *et al*. 2001, Qin and Gu 2004, Gu and Qin 2004, Chowdhury and Sarkar 2004, Mishra, *et al*. 2006, Chen, *et al*. 2006, Li, *et al*. 2003, Chen and Yu 2002). In most of the previous studies flutter derivatives were estimated mainly by free vibration techniques (Scanlan and Lin 1978, Sarkar 1994, Gu, *et al*. 2000, Gu, *et al*. 2001, Qin and Gu 2004, Gu and Qin 2004, Chowdhury and Sarkar 2004, Mishra, *et al*. 2006, Chen, *et al*. 2006, Li, *et al*. 2003, Chen and Yu 2002) and forced vibration techniques (Chen and Yu 2002). The forced vibration techniques are somewhat expensive since they involve sizeable equipment. The free vibration techniques seem to be more tractable than the forced vibration ones. However, at high reduced wind speeds, the vertical bending motion of the structure will decay rapidly due to the effect of positive vertical bending aerodynamic damping, and thus the length of time history available for system identification will decrease, which adds more difficulties to the system identification. Furthermore, the free vibration methods regard the buffeting forces and the responses as external noises, and it is, therefore, confronted with great difficulties at higher wind speeds due to the high "noises" (Gu, *et al*. 2000, Gu, *et al*. 2001). Both of the techniques are difficult to use in extracting flutter derivatives of bridge decks under simultaneous actions of wind and rain in the present test not only due to the methods themselves but also due to the requirements of rainproof facilities.

The stochastic system identification techniques (Qin and Gu 2004, Gu and Qin 2004, Mishra, *et al*. 2006) seem to be ideal for extracting flutter derivatives of bridge decks under simultaneous actions of wind and rain. The stochastic system identification techniques can directly extract the required dynamic parameters from the steady random responses of the bridge deck section model. In this kind of identification methods, the random aerodynamic loads are regarded as input rather than noise, which are more coincident with the fact, so the signal-to-noise ratio is not affected by wind speed, and the flutter derivatives at high reduced wind speeds can thus be available. These aspects give the stochastic system identification methods advantages over the deterministic methods in estimating the flutter derivatives of bridge decks, especially under wind and rain condition.

In this paper, a wind tunnel test on a quasi-streamlined thin plate model is carried out to investigate the differences between the flutter derivatives under conditions of only wind action and simultaneous actions of wind and rain, respectively. The formulation of Stochastic Subspace Identification (SSI in short), a kind of stochastic system identification method, whose effectiveness has been verified in Qin and Gu (2004), Gu and Qin (2004), is first presented. An experimental set-up is specially designed and manufactured to produce the condition of rain and wind. A wind tunnel test on the thin plate model is conducted under two kinds of conditions: only wind action; and simultaneous actions of wind and simulated rain. The flutter derivatives are then determined by SSI from its steady random vibration data. The comparison between the flutter derivatives of the thin plate model under the two different conditions tentatively indicates that rain has non-trivial effects on flutter derivatives, especially on A_2^*, and thus on flutter critical wind speeds of bridges.

2. Theoretical formulation of covariance-driven SSI (Qin and Gu 2004, Gu and Qin 2004)

The dynamic behavior of a bridge deck with two Degrees-Of-Freedom (DOF in short), i.e. h(bending) and α(torsion), in turbulent flow can be described by the following differential equations (Scanlan and Lin 1978):

$$\begin{aligned} m[\ddot{h}(t) + 2\xi_h\omega_h\dot{h}(t) + \omega_h^2 h(t)] &= L_{se}(t) + L_b(t) \\ I[\ddot{\alpha}(t) + 2\xi_\alpha\omega_\alpha\dot{\alpha}(t) + \omega_\alpha^2\alpha(t)] &= M_{se}(t) + M_b(t) \end{aligned} \tag{1}$$

where m and I are the mass and mass moment of inertia of the deck per unit span, respectively; ω_i is the natural frequency; ξ_i is the modal damping ratio ($i=h$, α); L_{se} and M_{se} are the self-excited lift and moment, respectively; while L_b and M_b are the buffeting lift and moment. The self-excited lift and moment are given as follows:

$$\begin{aligned} L_{se} &= \rho U^2 B\left[K_h H_1^*(K_h)\frac{\dot{h}}{U} + K_\alpha H_2^*(K_\alpha)\frac{B\dot{\alpha}}{U} + K_\alpha^2 H_3^*(K_\alpha)\alpha\right] \\ M_{se} &= \rho U^2 B^2\left[K_h A_1^*(K_h)\frac{\dot{h}}{U} + K_\alpha A_2^*(K_\alpha)\frac{B\dot{\alpha}}{U} + K_\alpha^2 A_3^*(K_\alpha)\alpha\right] \end{aligned} \tag{2}$$

where ρ is air mass density; B is the width of the bridge deck; U is the mean wind speed at the bridge deck level; $K_i=\omega_i B/U$ is the reduced frequency ($i=h$, α); and H_i^* and A_i^* ($i=1, 2, 3$) are the so-called flutter derivatives, which can be regarded as the implicit functions of the deck's modal parameters. The definitions of the buffeting lift and moment can be found from (Scanlan 1977).

By moving L_{se} and M_{se} to the left side, and merging the congeners into column vectors or matrices, Eq.(1) can be rewritten as follows:

$$[M]\{\ddot{y}(t)\} + [C^e]\{\dot{y}(t)\} + [K^e]\{y(t)\} = \{f(t)\} \tag{3}$$

where $\{y(t)\} = \{h(t)\ \alpha(t)\}^T$ is the generalized buffeting response; $\{f(t)\} = \{L_b(t)\ M_b(t)\}^T$ is the generalized aerodynamic force; $[M]$ is the mass matrix; $[C^e]$ is the gross damping matrix, i.e., the sum of the mechanical and aerodynamic damping matrices; and $[K^e]$ is the gross stiffness matrix. The flutter derivatives of bridge decks can be solved by stochastic system identification techniques.

Let

$$\begin{aligned} [A_c] &= \begin{bmatrix} O & I \\ -M^{-1}K^e & -M^{-1}C^e \end{bmatrix} \\ [C_c] &= [I \quad O] \end{aligned} \tag{4}$$

and

$$\{x\} = \begin{Bmatrix} y \\ \dot{y} \end{Bmatrix} \tag{5}$$

then Eq. (3) is transformed into the following stochastic state equations

$$\begin{cases} \{\dot{x}\} = [A_c]\{x\} + \{w\} \\ \{y\} = [C_c]\{x\} + \{v\} \end{cases} \tag{6}$$

The discrete form of Eq. (6) can be written as

$$\begin{cases} \{x_{k+1}\} = [A]\{x_k\} + \{w_k\} \\ \{y_k\} = [C]\{x_k\} + \{v_k\} \end{cases} \tag{7}$$

where $[A]$, $[C]$ and $\{x\}$ are known as state matrix, output shape matrix and state vector, respectively; $\{w_k\}$ and $\{v_k\}$ are the input and output noise sequences, respectively. Subscript $^*k$ denotes the value of * at time $k\Delta t$, where Δt means the sampling interval. O and I are the zero and identity matrices, respectively.

It is common to assume that $\{x_k\}$, $\{w_k\}$ and $\{v_k\}$ in Eq. (7) are mutually independent and hence

$$E[x_k w_k^T] = O \quad E[x_k v_k^T] = O \tag{8}$$

Defining

$$\begin{aligned} \Sigma &= E[x_k x_k^T] & Q &= E[w_k w_k^T] \\ \Lambda_i &= E[y_{k+i} y_k^T] & R &= E[v_k v_k^T] \\ G &= E[x_{k+i} y_k^T] & S &= E[w_k v_k^T] \end{aligned} \tag{9}$$

then we get the following Lyapunov equations for the state and output covariance matrices

$$\begin{aligned} \Sigma &= A\Sigma A^T + Q \\ \Lambda_0 &= C\Sigma C^T + R \\ G &= A\Sigma C^T + S \end{aligned} \tag{10}$$

From Eqs. (7), (8) and (9), the following equations can be deduced.

$$\Lambda_1 = E[\{y_{k+1}\}\{y_k\}^T] = E[(C\{x_{k+1}\} + \{v_{k+1}\})\{y_k\}^T] = E[C\{x_{k+1}\}\{y_k\}^T] = CG \tag{11}$$

$$\begin{aligned} \Lambda_1 &= E[\{y_{k+2}\}\{y_k\}^T] = E[(C\{x_{k+2}\} + \{v_{k+2}\})\{y_k\}^T] = E[C\{x_{k+2}\}\{y_k\}^T] = CE[\{x_{k+2}\}\{y_k\}^T] \\ &= CE[(A\{x_{k+1}\} + \{w_k\})\{y_k\}^T] = CE[A\{x_{k+1}\}\{y_k\}^T] = CAE[\{x_{k+1}\}\{y_k\}^T] = CA^{2-1}G \end{aligned} \tag{12}$$

and

$$\Lambda_i = CA^{i-1}G \tag{13}$$

Defining a block Toeplitz $T_{1|i}$ as

$$T_{1|i} = \begin{bmatrix} \Lambda_i & \Lambda_{i-1} & \dots & \Lambda_1 \\ \Lambda_{i+1} & \Lambda_i & \dots & \Lambda_2 \\ \vdots & \vdots & \vdots & \vdots \\ \Lambda_{2i-1} & \Lambda_{2i-2} & \dots & \Lambda_i \end{bmatrix} \tag{14}$$

one can infer from the definition of covariance matrix that $T_{1|i}$ can be expressed as the product of two block Hankel matrices Y_f and Y_p

$$T_{1|i} = Y_f Y_p^T \tag{15}$$

where Y_f and Y_p are composed of the 'Future' and 'Past' measurements, respectively.

$$Y_f = \frac{1}{\sqrt{j}} \begin{bmatrix} y_i & y_{i+1} & \cdots & y_{i+j-1} \\ y_{i+1} & y_{i+2} & \cdots & y_{i+j} \\ \vdots & \vdots & \vdots & \vdots \\ y_{2i-1} & y_{2i} & \cdots & y_{2i+j-2} \end{bmatrix} \qquad Y_p = \frac{1}{\sqrt{j}} \begin{bmatrix} y_0 & y_1 & \cdots & y_{j-1} \\ y_1 & y_2 & \cdots & y_j \\ \vdots & \vdots & \vdots & \vdots \\ y_{i-1} & y_i & \cdots & y_{i+j-2} \end{bmatrix} \tag{16}$$

In a manner similar to the classical Eigensystem Realization Algorithm (ERA in short) (Qin and Gu 2004), one can find

$$A = o_i^{+} T_{2|i} \varsigma_i = S_N^{-1/2} U^T T_{2|i} V S_N^{-1/2} \tag{17}$$

where N is model order, i.e. the maximum number of modes to be computed. U, S and V are matrices derived from the Singular-Value-Decomposition (SVD in short) of matrix $T_{1|i}$

$$T_{1|i} = USV^T \tag{18}$$

and

$$T_{2|i} = \begin{bmatrix} C \\ CA \\ \vdots \\ CA^{i-1} \end{bmatrix} A[A^{i-1}G \quad A^{i-2}G \quad \dots \quad AG \quad G] = o_i A \varsigma_i \tag{19}$$

Therefore, the modal parameters can be determined by solving the eigenvalue problem of state matrix A. By now, the theoretical formulation of covariance-driven SSI has been achieved.

According to Eqs. (15)~(18), a different combination of i, j and N will give a different state matrix, and thus a different pair of modal parameters. Therefore modal parameters should be derived from a series of combinations, rather than a single combination. In the process of identification, N or i should be given in series for certain j to get the frequency stability chart.

Once the modal parameters are identified, the gross damping matrix C^e and the gross stiffness matrix K^e in Eq. (3) can be readily determined by the pseudo-inverse method.

Let

$$\begin{aligned} \bar{C}^e &= M^{-1} C^e \qquad & \bar{K}^e &= M^{-1} K^e \\ \bar{C} &= M^{-1} C^0 \qquad & \bar{K} &= M^{-1} K^0 \end{aligned} \tag{20}$$

where C^0 and K^0 are the 'inherent' damping and stiffness matrices, respectively. Thus the flutter derivatives can be extracted from the following equations

$$
\begin{aligned}
H_1^*(k_h) &= -\frac{m}{\rho B^2 \omega_h}(\bar{C}_{11}^e - \bar{C}_{11}) \\
A_1^*(k_h) &= -\frac{I}{\rho B^3 \omega_h}(\bar{C}_{21}^e - \bar{C}_{21}) \\
H_2^*(k_\alpha) &= -\frac{m}{\rho B^3 \omega_\alpha}(\bar{C}_{12}^e - \bar{C}_{12}) \\
A_2^*(k_\alpha) &= -\frac{I}{\rho B^4 \omega_\alpha}(\bar{C}_{22}^e - \bar{C}_{22}) \\
H_3^*(k_\alpha) &= -\frac{m}{\rho B^3 \omega_\alpha^2}(\bar{K}_{12}^e - \bar{K}_{12}) \\
A_3^*(k_\alpha) &= -\frac{I}{\rho B^4 \omega_\alpha^2}(\bar{K}_{22}^e - \bar{K}_{22})
\end{aligned}
\tag{21}
$$

3. Wind tunnel test

3.1. Outline of the test

For convenience of the rain simulation, the present test was conducted in the efflux section of TJ-1 Boundary Layer Wind Tunnel in Tongji University, a straight-through boundary layer wind tunnel with an original working section of 1.8 m (width) × 1.8 m (height). The final diffuser of the wind tunnel was replaced by a new contraction section which was specially designed and manufactured to improve the quality of the wind field of the new testing section. The exit of the contraction section was a round one of 2.4 m diameter; and the maximum wind speed available was about 20 m/s. In fact, even if there was a contraction section at the end of the wind tunnel the uniformity of mean wind speed of the present testing section is not comparable to that of the original working section of the wind tunnel. The distance between the central section and the wind tunnel exit was 3 m. Fig. 1 shows the mean wind speeds at the different measuring points of the central section of the testing area. The data in the brackets are the relative differences between the testing wind speeds at the measuring points and the mean wind speed of all the measuring points (10.6 m/s). The wind speed at the central point of the section was 9.6 m/s, the lowest one for all the measuring points, and the maximum wind speed at another measuring point was about 12 m/s. The maximum relative difference between the wind speed at the central point and the mean one was about 13%. Even so, because this is only a comparison study for investigating the difference between the flutter derivatives of the model under two different conditions as is mentioned above, the unsatisfied wind field is still feasible for the present study. Moreover, the turbulent intensities at different positions were from 10% to 14.5%. A thin plate model (see Fig. 2) made of wood was adopted as the investigated model. The length, width and thickness of the model were 1.6, 0.45 and 0.022 m, respectively; the mass and inertial moment of mass per unit length were 9.3755 kg/m and 0.2502 kgm^2/m, respectively. The vertical bending and torsional frequencies of the model were

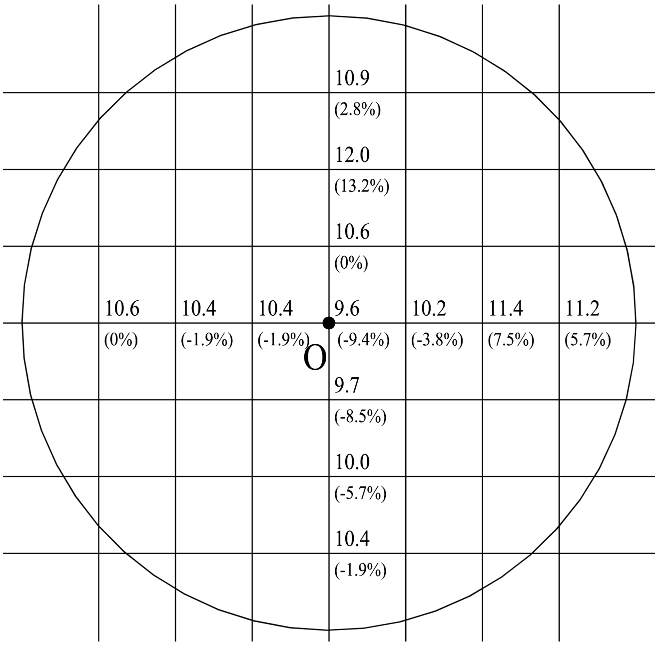

Fig. 1 Distributions of mean wind speeds of two sections

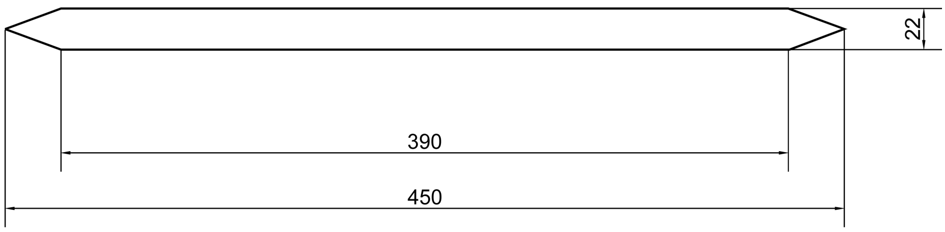

Fig. 2 Cross section of the streamlined thin plate model (unit: mm)

measured to be 1.75 Hz and 2.76 Hz, respectively, the torsion-vertical bending frequency ratio being 1.58. The damping ratio of the model was about 0.5%. In order to prevent rain from soaking the wood model, the model was painted with several coats of clear lacquer.

The new experimental set-up (see Fig. 3) was specially designed for the tests. The testing model was suspended with eight springs to the frame. To simulate a bridge section model with 2-DOFs, i.e., vertical bending and torsion, piano wires were used to arrest the motion of the model in longitudinal direction (see Fig. 4). The rain-simulating unit of the experimental set-up included a water pool, a lift pump, a valve and a sprinkler with sixteen sprinkling heads. The required rainfall and direction could be archived using the rain-simulating unit. Two kinds of rain rates of about 10.2 mm/hour and about 12 mm/hour were simulated for the test. Unfortunately, up to now there has been no research on the simulation law of rain in wind tunnel tests, so the rain rates were tentatively determined in the test. Moreover, because this paper is a comparison study to investigate whether rain has effects on the flutter derivatives, as is mentioned above, the rain rates seem to be feasible for the present study. The testing wind speed ranged from 4 to 11 m/s with the increment of 1 m/s.

Three piezoelectric accelerometers were mounted to the connecting rods at the ends of the model

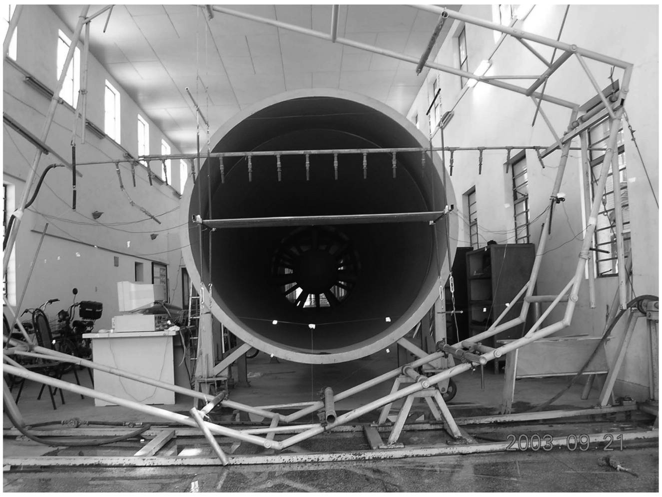

Fig. 3 Photograph of the testing system

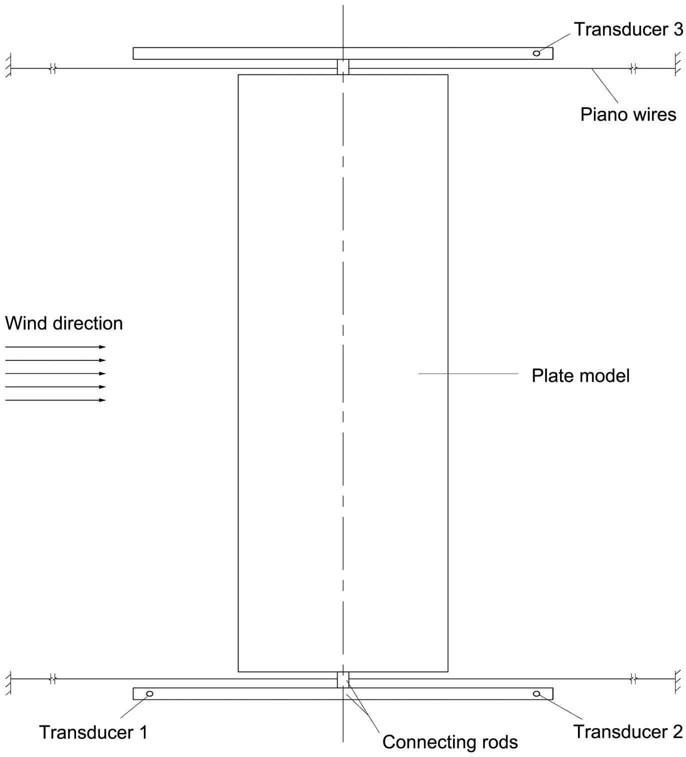

Fig. 4 Top view of the thin plate model

(see Fig. 4) to capture the vertical bending and torsion acceleration signals. The recording time of the vibration signal for each testing condition was 20 minutes. The response signals were sampled at a rate of 100 Hz. The sampled data for each of the testing condition were then divided into four groups, each of which had 30,000 sampling points. Four groups identified flutter derivatives were finally averaged to reduce the errors from the test.

The vertical and torsional components of the steady random buffeting response of the model can be respectively obtained by

$$h = \frac{x_1 + x_3}{2} \qquad \alpha = \frac{x_1 - x_2}{2l} \tag{22}$$

where x_1, x_2 and x_3 are the measurements from the accelerometers 1, 2 and 3, respectively (see Fig. 4); $2l$ is the space between transducer 1 and transducer 2.

3.2. Identified results

The covariance-driven SSI technique is here used to identify the modal parameters and further flutter derivatives from the above data. Perhaps due to the small difference of these two kinds of simulated rainfall, as mentioned above, the modal parameters and the identified flutter derivatives for the two rainfall conditions are almost the same, so the corresponding results for each of the two kinds of rainfall conditions are finally averaged to give mean values.

The variations of the modal parameters, i.e., total vertical bending and torsional damping ratios and frequencies, of the plate model under conditions of only wind action and simultaneous actions of wind and rain with reduced wind speeds are presented in Figs. 5 and 6. The total damping ratio here equals to the sum of the structural damping ratio and aerodynamic one; and the total frequency is also the same. An obvious difference between the torsional damping, a critical factor concerning flutter critical wind velocity of bridges, for the two kinds of conditions can be seen in Fig. 5. At the reduced wind speed of about 18, the total torsional damping ratio under the only wind condition is about 0.0028; while under the rain-wind condition it is about 0.011, nearly four times as large as that under only wind condition. On the other hand, from the below discussion it can also be seen that rain has great effects on the flutter derivatives A_2^* and H_2^*, reflecting torsion aerodynamic damping on torsional and vertical vibrations, respectively. The two circumstances hold identical tendencies. The difference between the total vertical bending damping ratios for the two conditions is much smaller than that between the torsional ones, with a mean difference between 15% and 20% for the reduced

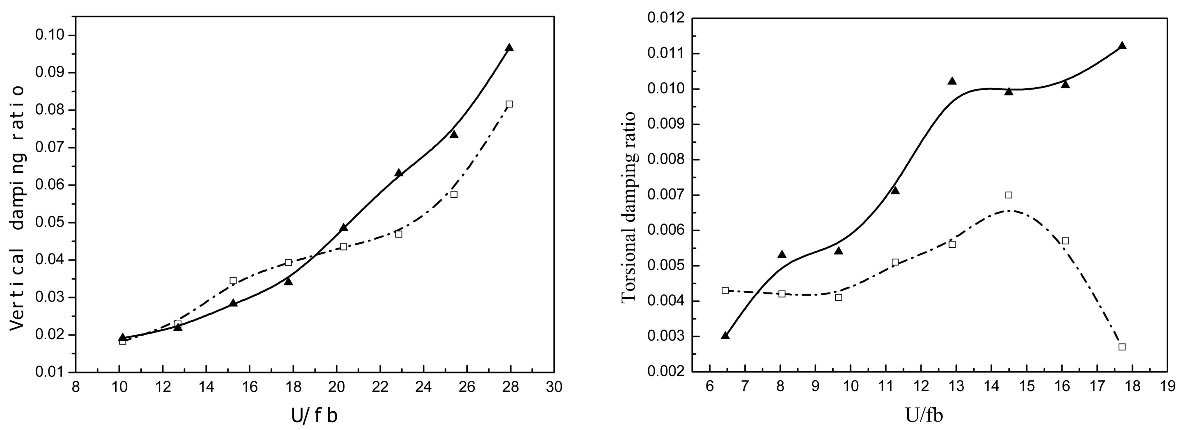

Fig. 5 Variation of damping ratios of the model with wind speed
(□ -- Only wind condition; ▲ -- Rain-wind condition)

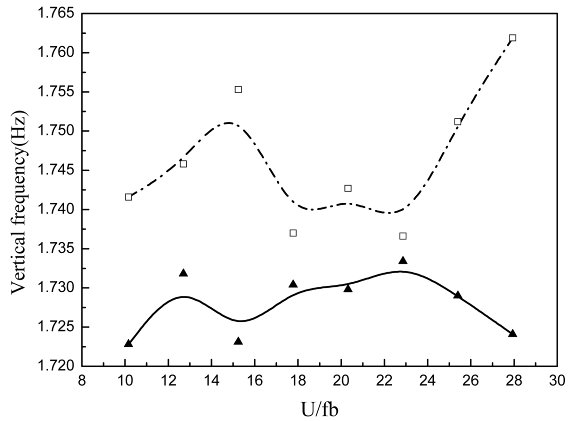

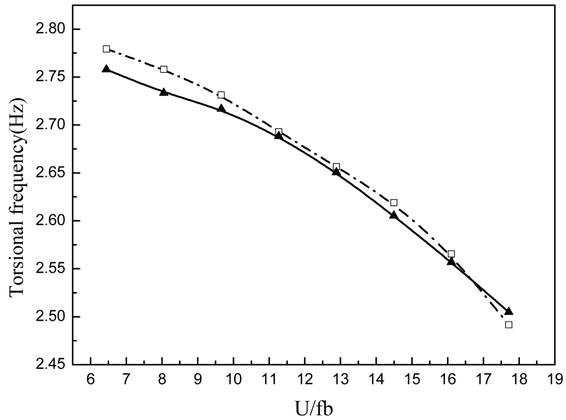

Fig. 6 Variation of frequencies of the model with wind speed
(□ -- Only wind condition; ▲ -- Rain-wind condition)

wind speeds larger than 21. Besides, the vertical bending frequency is also affected by rain to some extent; while the effect of rain on torsional frequency seems to be negligible.

Fig. 7 shows the identified flutter derivatives of the thin plate model under the two different conditions. The flutter derivatives of the thin plate model under only wind condition shown in the figure are obviously different from the theoretical solutions of an ideal thin plate (Scanlan and Tomko 1971) perhaps due to the ununiform wind field. Thus, only the identified flutter derivatives under only wind condition and rain-wind condition rather than the theoretical solutions are presented in Fig. 7 for the investigation of effect of rain on flutter derivatives of bridges. Under the simultaneous actions of rain and wind, the direct flutter derivative H_1^*, which reflects the effect of vertical bending aerodynamic damping on vertical vibration of the model, and cross flutter derivative A_1^*, reflecting the effect of vertical bending aerodynamic damping on torsion vibration, are somewhat different from those under only wind condition. The effects of rain on the other derivatives H_3^* and A_3^*, reflecting torsion aerodynamic stiffness on vertical and torsional vibrations, respectively, seem negligible. But it should be noted that the final two flutter derivatives A_2^* and H_2^*, reflecting torsion aerodynamic damping on torsional and vertical vibrations, respectively, are affected seriously by rain. This coincides with the result shown in Fig. 5(b), which indicates an obvious difference between the torsional damping for the two kinds of conditions, as is mentioned above. With the increase of wind speed, the absolute value of A_2^* of the thin plate model for the rain-wind condition increases more rapidly than that for the only wind condition. That is to say, the difference between A_2^* under only wind action and rain-wind action becomes larger with the increase of wind speed. The absolute value of A_2^* under rain-wind condition is about 2 times as large as that under only wind condition for the reduced wind velocity of 15. As is well known, A_2^* is the most important parameter for critical flutter wind velocity of bridges. Such large difference of A_2^* under the two different conditions indicates that rain will have great effects on the critical flutter wind speed of long-span bridges.

Since flutter is considered to be the result of self-excitation due to the steady component of wind, intense rain drops would be thought buffeting action on bridge decks. But there seems no evidence of the buffeting mechanism from the wind tunnel test results. And furthermore, it presently seems difficult to explain the mechanism of the effects of rain on the flutter derivatives in the way stated above. As is mentioned above this paper is just to investigate whether rain has effects on the flutter

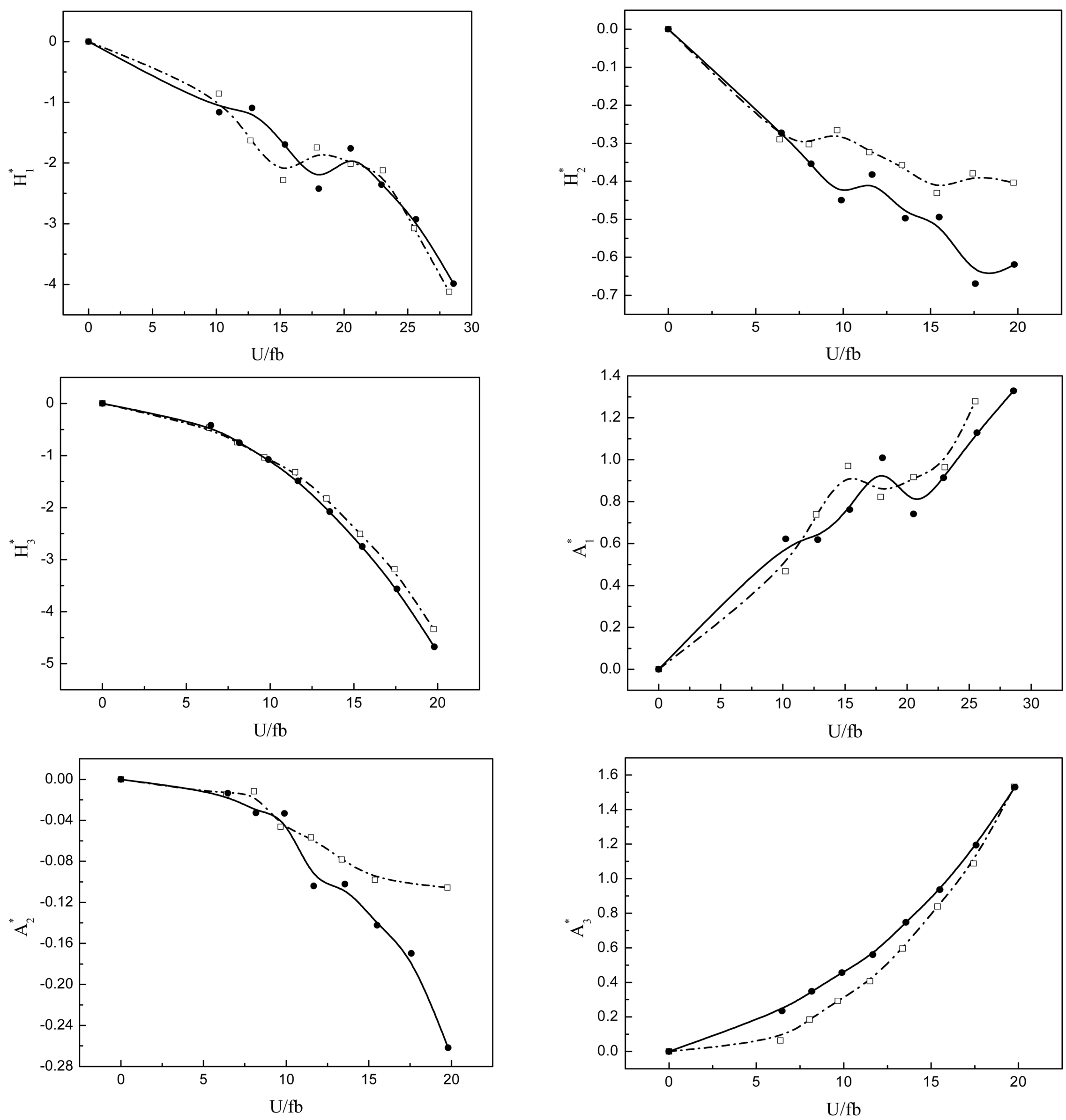

Fig. 7 Identified flutter derivatives under the two different conditions
(□ -- Only wind condition; ● -- Rain-wind condition)

derivatives of bridge decks, and the answer is yes. Further deepgoing studies on this subject will be made by the authors.

4. Concluding remarks

This paper makes an initial study on the effects of rain on flutter derivatives of long-span bridge decks. Wind tunnel tests on a quasi-streamlined thin plate model are conducted under only wind condition and under proper wind and rain conditions, respectively. The flutter derivatives are then extracted by the covariance-driven stochastic subspace identification technique from the steady random responses of the model. The comparison results tentatively indicate that rain has non-trivial effects on flutter derivatives, especially has great effects on the total torsional damping and thus the torsional damping-related flutter derivatives, H_2^* and A_2^*. Large difference of A_2^* under the two different conditions indicates that rain will have great effects on the critical flutter wind speed of long-span bridges.

Although the present testing results show the non-trivial effects of rain on flutter derivatives of bridge decks, it is difficult to explain the mechanism and further to give a proper theoretical description of the phenomenon. Experimental and theoretical studies on effects of rain on wind loads of bridges and the other kinds of structures, such as tall buildings and large-span roofs, will be further performed.

Acknowledgement

The authors would like to gratefully acknowledge the support of the National Natural Science Foundation of China (50621062).

References

Gu, M. and Lu, Q. (2001), "Theoretical analysis of wind-rain induced vibration of cables of cable-stayed bridges", *J. Wind Eng., APCWE-V*, **89**, 125-128.

Scanlan, R. H. and Lin, W.H. (1978), "Effects of turbulence on bridge flutter derivatives", *J. Eng. Mech., ASCE*, **104**(4), 719-333.

Sarkar, P. P. (1994), "Identification of aeroelastic parameters of flexible bridges", *J. Eng. Mech., ASCE*, **120**(8), 1718-1741.

Gu, M., Zhang, R. X. and Xiang, H. F. (2000), "Identification of flutter derivatives of bridge decks", *J. Wind Eng. Ind. Aerodyn.*, **84**, 151-162.

Gu, M., Zhang, R. X. and Xiang H. F. (2001), "Parametric study on flutter derivatives of bridge decks", *Eng. Struct.*, **23**, 1607-1613.

Qin, X. R. and Gu, M. (2004), "Determination of flutter derivatives by stochastic subspace identification technique", *Wind Struct.*, **7**(3), 173-186.

Gu, M. and Qin, X. R. (2004), "Direct identification of flutter derivatives and aerodynamic admittance of bridge decks from structural random response", *Eng. Struct.*, **26**(14), 2161-2172.

Chowdhury, A. G. and Sarkar, P. P. (2004), "Identification of eighteen flutter derivatives of an airfoil and a bridge deck", *Wind Struct.*, **7**(3), 187-202.

Shambhu Sharan Mishra, Krishen Kumar and Prem Krishna (2006), "Identification of 18 flutter derivatives by covariance driven stochastic subspace method", *Wind Struct.*, **9**(2), 159-178.

Chen, A. R., Xu, F. Y. and Ma, R. J. (2006), "Identification of flutter derivatives of bridge decks using stochastic search technique", *Wind Struct.*, **9**(6), 441-455.

Li, Y. L., Liao, H. L. and Qiang, S. Z. (2003), "Weighting ensemble least-square method for flutter derivatives of bridge decks", *J. Wind Eng. Ind. Aerodyn.*, **91**(6), 713-721.

Chen, Z. Q. and Yu, X. D. (2002), "A new method for measuring flutter self-excited forces of long-span bridges" (in Chinese), *China Civil Eng. J.*, **35**(5), 34-41.

Scanlan, R. H. (1977), "Motion of suspended bridge spans under gusty wind", *J. Struct. Eng. Div., ASCE*, **103**(9), 1867-1883.

Scanlan, R. H. and Tomko J. J. (1971), "Airfoil and bridge deck flutter derivatives", *J. Eng. Mech. Div., ASCE*, **97**(6), 1717-1733.

CC